

초음속 마이크로제트 유동특성에 관한 연구

신춘식* · 김희동** · Toshiaki Setoguchi***

A Study on the Flow Characteristics of Supersonic Microjets

Choon-Sik Shin* · Heuy-Dong Kim** · Toshiaki Setoguchi***

ABSTRACT

Supersonic microjets acquire considerable research interest from a fundamental fluid dynamics perspective, in part because the combination of highly compressible flow at low-to-moderate Reynolds number is not very common, and in part due to the complex nature of the flow itself. In addition, microjets have a great variety engineering applications such as micro-propulsion, MEMS (Micro-Electro Mechanical Systems) components, microjet actuators and fine particle deposition and removal. Numerical simulations have been carried out at moderate nozzle pressure ratios and for different nozzle exit diameters to investigate and to understand in-depth of aerodynamic characteristics of supersonic microjets.

Key Words: Compressible Flow(압축성 유동), Microjets(마이크로제트), Supersonic(초음속), Jet Structure(제트 구조), Numerical Simulation(수치 시뮬레이션)

1. INTRODUCTION

Microjets acquire considerable research interest due to their potential use in various engineering applications such as micro-propulsion, MEMS components, and fine particle deposition and removal. Supersonic microjets provide several advantages over subsonic jets in a number of applications. Microjets are also used as actuators to control the ground effect created by large supersonic impinging jets, typically occur in STOVL (Short Take-off and Vertical Landing) aircraft during hover. More recently, micro-jet actuators have also been used for controlling

the flow separations, cavity flows, jet noise, and for suppressing turbulence in jet flows. In addition, the flowfield of microjets is also of interest from a fundamental fluid dynamics perspective, in part because the combination of highly compressible flow at low-to-moderate Reynolds number is not very common, and in part due to the complex nature of the flow itself. The present study pertains with numerical simulations of supersonic microjets at moderate nozzle pressure ratios. Especially, we focused on the effect of nozzle exit diameter on the aerodynamic characteristics of microjets.

2. NUMERICAL SIMULATION

The two-dimensional viscous flow solver, developed at our laboratory, is used for these computations. It is based on the compressible

* 안동대학교 대학원 기계공학과

** 안동대학교 기계공학부

연락처, E-mail: kimhd@andong.ac.kr

*** 일본 Saga대학교 기계공학과

Reynolds and Favre-averaged Navier-Stokes equations, and modified Goldberg's k-R turbulence model [1] is used for closure. The governing equations are non-dimensionalized with reference values at the inlet conditions upstream of the nozzle written in an axisymmetric coordinate system. The 3rd order TVD (Total Variation Diminishing) finite difference scheme with MUSCL approach [2] is used to discretize the spatial derivatives, a second order-central difference scheme for the viscous terms, and a second-order fractional step is employed for time integration.

Axisymmetric supersonic microjets flow driven by the sonic nozzle [3] with exit diameters of $\phi D_e = 400 \mu\text{m}$, $200 \mu\text{m}$ and $100 \mu\text{m}$ (characteristic length) are considered in the present computation, as shown in Fig.1. The dry air as working gas is issued from that sonic nozzle. The resulting number of grids applied is 50×60 in the nozzle region and 200×111 in the jet plume region.

In the present study, three nozzle pressure ratios, the ratio of the reservoir pressure p_0 (atmospheric pressure) to back pressure p_b ($= p_0/p_b$), used are 4.57, 5.23 and 6.2, respectively. Total temperature T_0 , total pressure p_0 in the reservoir are 298.15 K, 101.3 kPa, respectively.

3. RESULTS AND DISCUSSION

3.1 Comparison with Experimental Results

The comparisons of predicted iso-density contour with schlieren photograph obtained by experiment for $p_0/p_b = 6.2$, is shown in Fig. 2. The sonic nozzle [3] with exit diameters of $\phi D_e = 12.7 \text{ mm}$ are used in the computation and experiment. The jet is underexpanded at the nozzle exit and barrel shocks are formed due to the differences in pressure between the underexpanded gas and the ambient gas. Therefore, these shocks reflect from the jet axis. Consequently the Mach disk is formed near the

jet axis. At the intersection of the Mach disk with the barrel shock, a triple-point is formed. In the downstream of the triple-point the slip line is observed. The predicted iso-density contour is nearly same as the experimentally visualized result. Furthermore, the predicted Mach disk location and diameter are $L_m/D_e = 1.5613$ and $D_m/D_e = 0.5394$, respectively, while the experimental values are 1.5646 and 0.5264, respectively. Here, location of Mach disk is measured from the nozzle exit, and both the location and diameter of the Mach disk are normalized by nozzle exit diameter. Thus, the present computational works predict well the flow structures of the highly underexpanded supersonic jets.

3.2 Structure of Supersonic Microjets

Computer schlieren images of the supersonic underexpanded jets from the nozzle with $100 \mu\text{m}$ of exit diameter at pressure ratios of 4.57, 5.23 and 6.2 are shown in Fig. 3(a-c). Similarly, Figs.

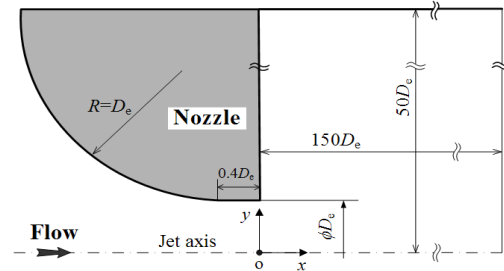


Fig. 1. Computational domain

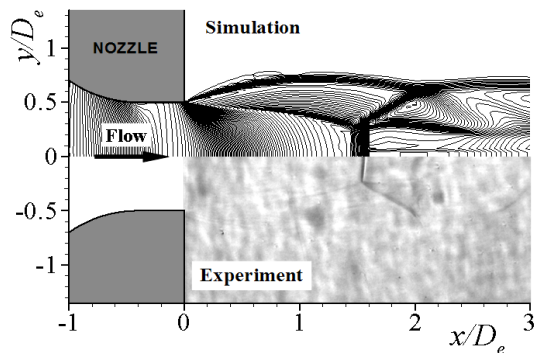


Fig. 2. Comparison of the present computation with experiment ($p_0/p_b = 6.2$)

4(a-c) and 5 (a-c) show the flowfields for the 200 μm and 400 μm , respectively. In these figures, the jet flowfields evolve from weak underexpansion to strong underexpansion.

The jet is in moderately underexpanded condition, at lower nozzle pressure ratio p_0/p_b , the oblique shocks almost crosses on the jet axis. However, as the jet underexpansion ratio increases, central Mach disk appears near the jet axis. The presence of such Mach disks is clearly visible in Figs. 3(c), 4(c) and 5(b, c). At triple-point the oblique shock, the Mach disk, and the rear shock are confluences and leads to a characteristic lambda (Λ) shock structure. The velocity difference between the fluid streams that pass above and below this triple-point results in a shear layer or slip line. These slip lines emanating from the triple-point can be seen in Figs. 3(c), 4(c) and 5(b, c).

3.3 Surveys of Jet Centerline Pressure

The static pressure distributions downstream of the nozzle exit are strongly dependent on the nozzle exit diameter i.e. on jet diameter. This fact can be confirmed from the numerically predicted static pressure distributions along jet centerline at a nozzle pressure ratio of 5.23 in Fig. 6. The location of the sharp jump in the static pressure distribution is slightly varied with the jet diameter. The centerline static pressure distributions for the 200 μm and 400 μm jets, are presented in Figs. 7(a) and (b). The pressures under each operating condition (p_0/p_b) exhibit unique characteristics. From Fig. 7(a), the variation in pressure shows the characteristic quasi-periodic structure, due to the presence of shock cells in the jet flow fields. Moreover, as the nozzle pressure ratio p_0/p_b is increased, the flow field is seen to stretch, where the shock cell spacing increases, leading to an increase in the length over which the shocks are present. At low p_0/p_b the oblique shocks cross in a normal fashion, which changes to irregular crossing as the p_0/p_b is increased.

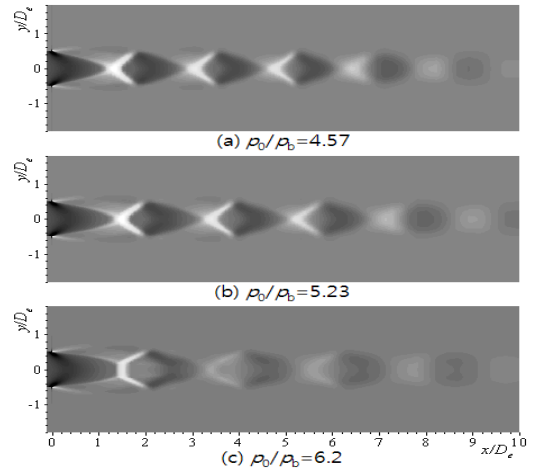


Fig. 3. Numerical schlieren images of 100 μm microjets

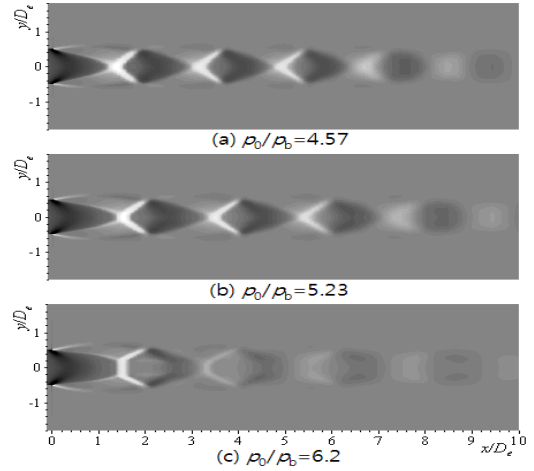


Fig. 4. Numerical schlieren images of 200 μm microjets

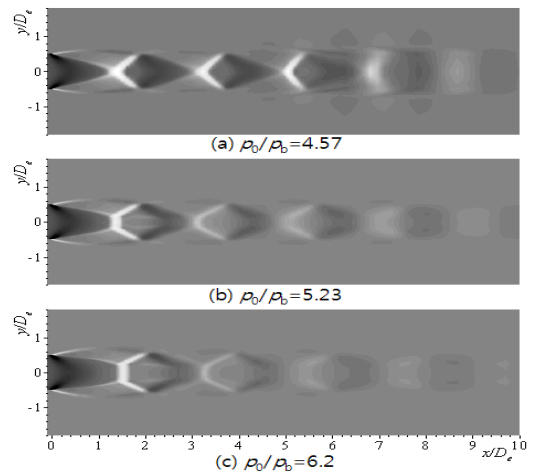


Fig. 5. Numerical schlieren images of 400 μm microjets

For 400 μm jet, the centerline pressure distributions displays characteristics very similar to 200 μm jet, as shown in Fig. 7(b). Furthermore, from Figs. 7(a) and (b), when the highly underexpanded condition is reached ($p_0/p_b=6.2$), a Mach disk is first visually observed at the end of the first shock cell. At

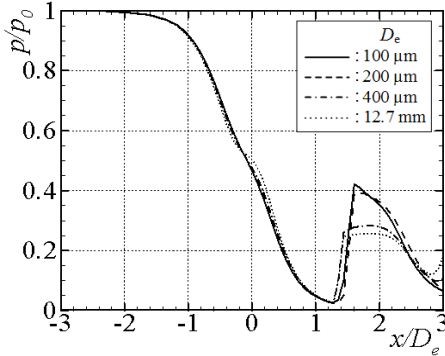
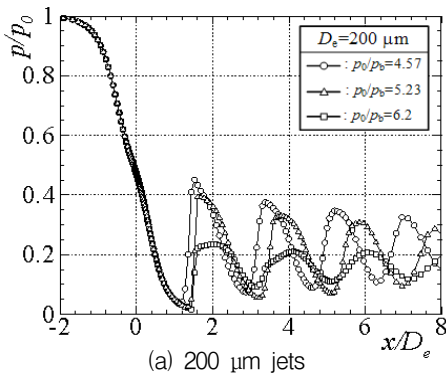
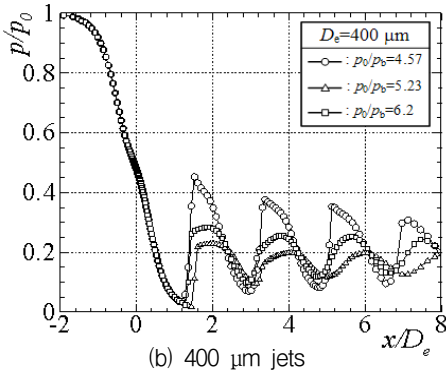


Fig. 6. Static pressure distributions along jet axis ($p_0/p_b=5.23$)



(a) 200 μm jets



(b) 400 μm jets

Fig. 7. Effect of nozzle pressure ratio on the static pressure distributions along jet axis

downstream of the first shock cell, the flow become subsonic, leading to a sudden drop in the pressure. The formation of Mach disk can also be clearly seen from the computer schlieren, in Figs. 3, 4 and 5.

4. CONCLUSION

In the present study, axisymmetric supersonic microjets flow was investigated numerically under different operating conditions (p_0/p_b). Results obtained are summarized as follows: The presence of shock cells in the jet flow fields exhibit the characteristic quasi-periodic structure in the jet centerline pressure distributions. Moreover, at highly underexpanded condition, the Mach disks can be clearly visualized at the end of the first shock cell and the jet flow field is seen to stretch, where the shock cell spacing increases. For a given pressure ratio, the jet diameter has a significant influence on the configuration of barrel shock and the diameter of Mach disk. Other hand, the configuration of jet boundary and the location of Mach disk is not so sensitive to the jet diameter, for a given p_0/p_b . However, significant influence was observed on the configuration of jet boundary and barrel shock under different operating conditions (p_0/p_b), and the microjet is expanded outward with p_0/p_b .

REFERENCES

1. Goldberg, U. C., "Toward a Pointwise Turbulence Model for Wall-Bounded and Free Shear Flows", Transactions of the ASME, Vol.116, pp.72~76, 1994.
2. Yee, H. C., "A class of high-resolution explicit and implicit shock capturing methods", NASA TM-89464, 1989.
3. Addy, A. L., "Effects of Axisymmetric Sonic Nozzle Geometry on Mach Disk Characteristics", AIAA Journal, Vol.19, No.1, 1981.